

# A ternary programmable dispersion matrix for receive/transmit optical beamforming

M. Jaeger<sup>a</sup>, S. Palit<sup>b</sup>, S. Granieri<sup>a</sup>, B.A. Black<sup>b</sup>, and A. Siahmakoun<sup>a</sup>

<sup>a</sup>Department of Physics and Applied Optics,

<sup>b</sup>Department of Electrical and Computer Engineering

Rose-Hulman Institute of Technology, Terre Haute, Indiana 47803, USA

## ABSTRACT

We present a new architecture for a programmable dispersion matrix for optical beamforming. A 2-channel prototype is constructed to demonstrate beam steering for angles of  $\pm 70^\circ$  in the receive/transmit mode in RF 0.1-1 GHz frequency range.

**Keywords:** Fiber optic link, beamformer, programmable dispersion matrix, true time delay, fiber Bragg grating

## 1. INTRODUCTION

High-resolution phased-array antennas are degraded by distortion introduced by electronic phase shifters. Pulse distortion and shifts in beam angle are experienced when the bandwidth is large or the operating frequency is changed. In such systems true-time delay (TTD) phase shifters eliminate these errors. In conventional RF systems, TTD is achieved by switching between different lengths of electrical cable. However, these implementations tend to be bulky, heavy, and susceptible to electromagnetic interference. The fiber-optic TTD systems provide benefits in these areas.

A variety of techniques have been proposed for obtaining TTD capability using fiber-optic systems<sup>1</sup>. In particular, systems using fiber Bragg gratings (FBG) for providing time delays have been proposed and demonstrated<sup>2,3</sup>. Two-bit and five-bit binary transmit/receive modules using FBG matrices have been demonstrated<sup>4,5</sup>.

In this paper we report on the design and experimental demonstration of a ternary architecture for a two-channel true-time delay programmable matrix for controlling a phased-array antenna. The wideband processor has a resolution of 31 delay configurations.

## 2. SYSTEM DESCRIPTION

A schematic drawing of the beamformer architecture in the transmit mode is shown in Fig. 1(a). Two laser diodes provide optical channels at wavelengths  $\lambda_1$  and  $\lambda_2$ . The two channels are multiplexed and externally modulated with an RF signal using an electrooptic modulator (EOM). Modulation of multiplexed channels ensures zero phase delay between the RF components before the optical signal is processed. The modulated carrier feeds a programmable dispersion matrix (PDM), which performs the true-time delay processing. For each configuration of the PDM,  $\lambda_1$  either leads or lags  $\lambda_2$  by a time period. At the output of the PDM, after the proper delay has been set, the channels are demultiplexed. Two broadband photodetectors recover the delayed RF signals that will feed the antenna elements.

The architecture of a four-delay-line PDM, which is based on fiber Bragg grating arrays, is shown in Fig. 2. The PDM is arranged in a ternary layout, so the RF signal modulating  $\lambda_1$  can either lead or lag the RF signal modulating  $\lambda_2$  in each line, allowing perfectly symmetrical beamforming. To achieve the same resolution using a binary configuration an additional line is required<sup>5</sup>. The  $2^N - 1$  delay configurations version of the two-channel ternary architecture consists of an array of  $N-1$  delay lines. Each delay line is constructed by splicing two FBGs. The center wavelength of each FBG matches one of the multiplexed optical channels. The separation between FBGs is different for each delay line. Thus,

time delay(s) between channels is proportional to these FBG separations. The separation of the two adjacent gratings for the  $i^{\text{th}}$  line is given by

$$\Delta L_i = 2^{i-1} \Delta L_1, \quad (1)$$

where  $\Delta L_1$  is the minimum separation between gratings in line 1. Using Eq. (1) the time delay provided by the  $i^{\text{th}}$  line can be written as  $t_i = \frac{2n_{\text{eff}} \Delta L_i}{c}$ , where  $n_{\text{eff}}$  is the effective refractive index of the fiber and  $c$  is the speed of light. Each of the  $2^N - 1$  delay configurations of the PDM can be represented as

$$t_m = \sum_{i=1}^{N-1} a_i \cdot t_i, \quad (2)$$

where the value of the constant  $a_i$  depends on the optical signal path. The optical signal can be routed to the bottom end or top end of each delay line, represented as  $a_i = 1$  and  $a_i = -1$  respectively. On other hand, when light is bypassing the delay line  $a_i = 0$ . The time delays, which are integer multiples of the delay  $t_1$ , range from  $-2^{N-1} \cdot t_1$  to  $2^{N-1} \cdot t_1$ , resulting in a symmetrically distributed delay configuration. Owing to the ternary setup, the value for  $a_i$  is not unique for a given time delay  $t_m$ . This property can be used to improve the performance of the system, i.e., for any desired time delay a combination of array lines is chosen that involves a minimum number of delay lines. The minimum time delay associated with line 1 is directly related to the angular resolution and the minimum steering angle of any beamformer<sup>6</sup>.

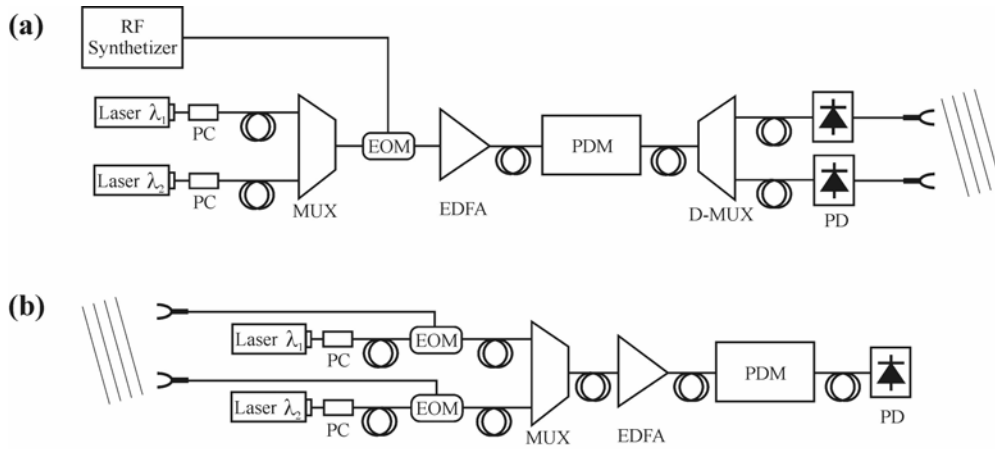


**Figure 1:** Beamformer setup configuration for: (a) transmit mode and (b) receive mode.

The steering (azimuth) angle  $q_m$  is related to a characteristic parameter of the PDM, that is  $t_1$ , and a geometrical parameter of the antenna, the transmit/receive element spacing  $\Lambda$ , by

$$q_m = \arcsin\left(\frac{c m t_1}{\Lambda}\right). \quad (3)$$

In Fig. 1(b) the schematic for the receive-mode configuration is shown. An incoming RF signal from a target is received by two antenna array elements. The phase difference at the antenna elements depends on the target angle. The received RF signals at the two elements respectively modulate two individual optical carriers. The time delay between the multiplexed optical channels is corrected by the PDM and detected with a single photodetector. The output power of the photodetector is a function of the corrected phase difference between the two RF signals

$$P(\text{dB}) = 10 \log(K_1 + K_2 \cos \Delta f), \quad (4)$$

where  $\Delta f$  is the phase difference and  $K_1, K_2$  are the proportionality constants. Thus, the output power is related to the target angular position via this phase difference. When the PDM properly corrects for the phase difference at the antenna elements a maximum power will be detected for the target position.

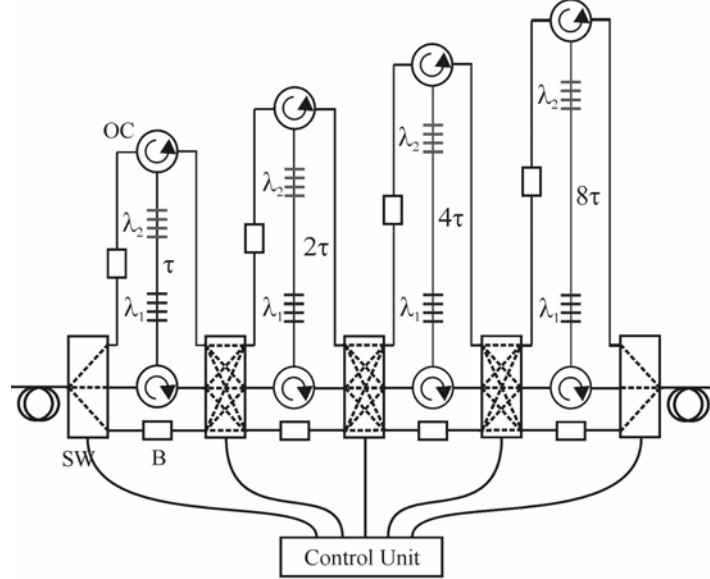


**Figure 2:** Two-channel ternary programmable dispersion matrix with 31 configurations. SW: optical switch, B: balancer, OC: optical circulator

### 3. EXPERIMENTAL RESULTS

Two 15 mW Alcatel A1905LMI semiconductor lasers, with wavelengths of 1551.7 nm and 1550.9 nm, provide optical carriers. Two in-fiber polarization controllers set proper polarization at the inputs of the 10 GHz SDL EOM. The experiment is performed using a PDM that provides 31 delay configurations. The central wavelengths of the fiber Bragg gratings match the frequencies of ITU channels 32 and 33 (100 GHz spacing). All the gratings have reflectivities from 94.8% to 99.3% and FWHM bandwidths of 0.5 nm. In each delay line, the first FBG (closer to the switches towards the bottom in Fig. (2)) reflects light of channel ITU 32 while the second FBG reflects light of channel ITU 33. Because of the ternary layout of the PDM, it is possible to send light from both sides into a given delay line; this produces “positive” and “negative” delays. Hence the 31 possible delay configurations are

$$t_m = m t_1, \quad m = -15, \dots, 15. \quad (5)$$

The minimum separation between FBGs is  $\Delta L_1 = 0.02$  m corresponding to line 1. Separations for successive lines are:  $\Delta L = 0.04$  m, 0.08 m and 0.16 m with an accuracy of  $\pm 1$  mm. The theoretical minimum time delay of the PDM, calculated from Eq. (2), is  $t_1 = 195.8$  ps. Optical circulators are used to route the signals to/from each line. In order to obtain all the delay configurations, four 3x3 switches are used. The switches are controlled by means of an Agilent 34970A data acquisition/Switch unit.

Note that the optical signals will undergo different levels of attenuation depending upon the delay configuration, i.e. the number of components in the optical path varies for each delay. Thus the insertion loss of the PDM is path dependent, leading to spurious power variations from changes in constants  $K_1$  and  $K_2$  associated with different configurations. In order to balance the optical power in the PDM, in-fiber air-gap mechanical attenuators are placed in each of the paths

that bypass the delay lines, as shown in Fig. 2. Since the attenuation change between “positive” ( $a_i = 1$ ) and “negative” ( $a_i = -1$ ) delay for each delay line is small, no correction for these attenuation differences is necessary. These differences are due to the slightly different insertion losses of the circulators used in the “positive” and “negative” paths.

Since the FBGs have different reflectivities, the in-line power of the individual optical carriers out of the system changes with different delay line combinations. To compensate for these changes, one of the lasers is coupled to an EXFO FVA3100 programmable optical attenuator, and its attenuation level is programmed to match the optical power of the other laser at the output of the system, for each delay configuration. After balancing, the total insertion loss of the system is approximately 36 dB. The main sources of loss are the EOM biased at quadrature (6-8 dB), the fiber connectors, and the optical circulators in the PDM. Thus, an IPG Photonics erbium doped fiber amplifier (EDFA) with 20 dB gain is placed after 2-channel multiplexer to improve the dynamic range of the system.

### 3.1 Beam pattern Characterization

For the transmit mode beam pattern characterization, the configuration shown in Fig. 1(a) is slightly modified. In this case the RF phase shift created by the PDM is transformed to power variations in a single photodetector, according to Eq. (4). In order to obtain the transmit beam pattern for a desired RF, the PDM is stepped through each of the 31 possible delay configurations. The modulator is fed with an amplified RF signal out of port #1 of a vector network analyzer, and port #2 of the network analyzer detects the RF signal out of the photodetector. The magnitude of s-parameter  $s_{21}$  is measured for each delay configuration for frequencies between 0.2 GHz and 1GHz.

Fig. 3(a) compares the experimental points with theoretical plots obtained from Eqs.(3) and (4) at RF values of 0.5 GHz and 1GHz. These are for a beam steering range of  $-70^\circ$  to  $+70^\circ$ , using  $\Lambda = 1$  m as the element spacing of the antenna-array. We attribute the discrepancies between the experimental points and the theoretical curves to the finite bandwidth of the FBGs of both channels. This causes some overlap between the reflectivity profiles, which in turn leads to power fluctuation due to crosstalk.

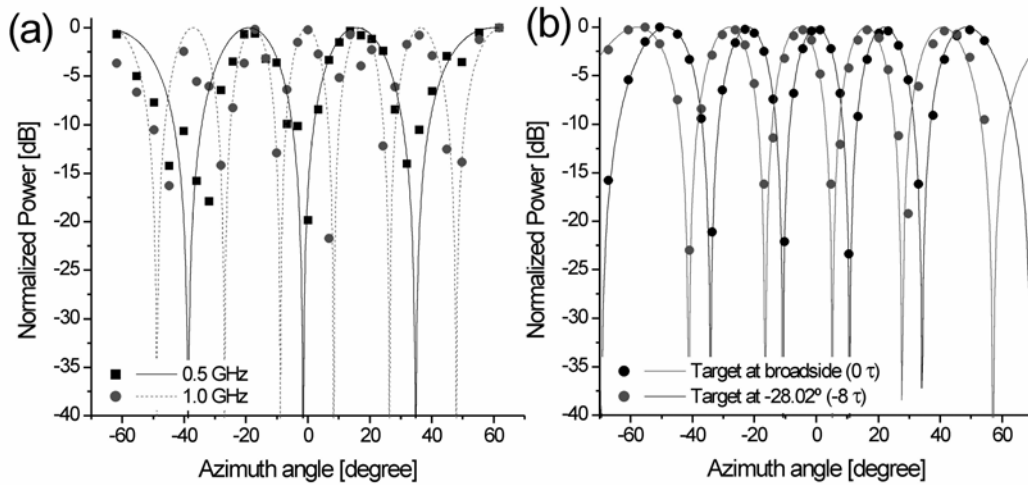


**Figure 3:** Beam patterns obtained in: (a) transmit mode at 0.5 GHz and 1 GHz; (b) receive mode at 0.8 GHz for target at broadside and  $-28.02^\circ$ .

For the receive-mode beam pattern characterization, an HP model 83650A RF synthesizer simulates an incoming RF signal from a target. This signal is split and sent to optical modulators shown in Fig. 1(b). A phase shifter introduced before one of the modulators simulates the phase difference between two antenna elements due to a non-broadside target.

Beam patterns are constructed by sweeping the RF phase shifter and measuring the RF output power from the single photodetector using the RF spectrum analyzer.

Fig. 3(b) illustrates beam patterns measured at an RF frequency of 0.5 GHz for two PDM delay configurations: zero and  $-15t_1$ . Fig. 4(a) shows the experimental azimuth angle of the mainlobe of the receive beam pattern for all 31 delay configurations. These compare well with the theoretical plot of Eq (3). Fig. 4(b) further demonstrates the “squint free” nature of the system. In this figure the experimental mainlobe position of the receive beam pattern for azimuth angles of  $-28.02^\circ$ ,  $0^\circ$ ,  $3.37^\circ$ ,  $6.74^\circ$ ,  $10.146^\circ$  and  $28.02^\circ$  are shown plotted against frequency.

#### 4. DISCUSSION AND CONCLUSIONS

We propose a ternary architecture PDM for optical beamforming. The main advantage over the binary counterpart is related to the angular resolution. The ternary architecture allows beam steering in a perfectly symmetrical angular range centered about the broadside position. For the same angular resolution the binary version requires an additional delay line in order to achieve the same performance.

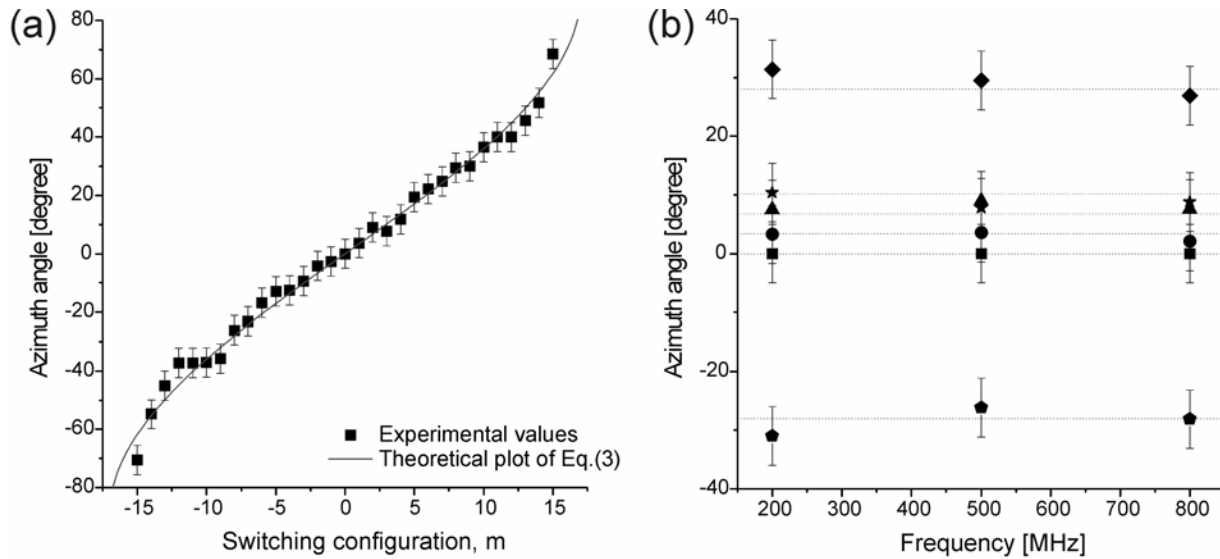


**Figure 4:** (a) Angular position of mainlobe in beam pattern for all possible configurations at 0.5 GHz. Solid line represents theoretical values of Eq. (3).

We have demonstrated and characterized a two-channel optical beamformer prototype operating at 1550nm using a ternary PDM. Such a system requires fewer switches than the binary version capable of feeding a phase array antenna with 31 different phase delays. The working prototype is used to demonstrate beam pattern measurements in the receive/transmit mode for the RF 0.1-1 GHz frequency range. These beam patterns are obtained for target positions at broad side and  $28.02^\circ$  for steering angles of  $\pm 70^\circ$ . Our optical beamformer exhibits a squint-free radiation pattern in the RF band of 0.2-1.0 GHz.

The use of FBGs and a WDM architecture to produce the appropriate time delay for each antenna element can be extended to enable processing of multiple simultaneous beams. A simple prototype for processing two independent simultaneous beams in a three-bit two-channel beamformer is currently under investigation and its development and preliminary results will be presented in the near future.

## REFERENCES

1. N. Riza, ed., *Selected papers on photonic control systems for phased array antennas*. SPIE Milestone Series, vol MS 136, Washington, 1997.
2. R. Soref, "Fiber grating prism for true time delay beamsteering," *Fiber and Integrated optics*, **15**, pp. 325-333, 1996.
3. H. Zmuda, A. Soref, P. Payson, S. Johns and E. Toughlian, "Photonic beamformer for phased array antennas using a fiber grating prism," *IEEE Photon. Technol. Lett.*, **9**, pp. 241-243, 1997.
4. D. Tong, and M. Wu, "Transmit/receive module of multiwavelength optically controlled phased-array antennas," *IEEE Photon. Technol. Lett.*, **10**, pp. 1018-1020, 1998.
5. S. Palit, S. Granieri, A. Siahmakoun, B. Black and C. Pagel, "Performance characteristics of 5-bit optical receive beamformer," *Proc. Photonics North 2002 Conf.* (in press).
6. B. Black, A. Siahmakoun, L. Slaybaugh, J. Chestnut and D. Thalen, "Component-level simulation of optical beamforming systems," *Proc. SPIE*, **4532**, pp. 494-499, 2001.